International Journal of Biochemistry and Cell Biology 98 (2018) 127–136

Contents lists available at ScienceDirect

International Journal of Biochemistry and Cell Biology

journal homepage: www.elsevier.com/locate/biocel

The kinetic analysis of the *N*-methylation of 4-phenylpyridine by nicotinamide *N*-methyltransferase: Evidence for a novel mechanism of substrate inhibition

Matthijs J. van Haren[a,1], Martin G. Thomas[b,1], Davide Sartini[c], David J. Barlow[b], David B. Ramsden[d], Monica Emanuelli[c], Fábio Klamt[e], Nathaniel I. Martin[a,*], Richard B. Parsons[b,*]

[a] Utrecht University, Utrecht Institute for Pharmaceutical Science, Universiteitsweg 99, 3584 CG Utrecht, The Netherlands
[b] King's College London, Institute of Pharmaceutical Science, 150 Stamford Street, London SE1 9NH, UK
[c] Universitá Politecnica delle Marche, Department of Clinical Sciences, School of Medicine, Ancona, Italy
[d] University of Birmingham, Institute of Metabolism and Systems Research, Edgbaston, Birmingham B15 2TH, UK
[e] Universidade Federal do Rio Grande do Sul, Departmento de Bioquímica, Instituto de Ciências Básicas de Saúde, Rua Ramiro Barcelos, Porto Alegre, RS 90035 003, Brazil

ARTICLE INFO

Keywords:
Enzyme kinetics
Neurotoxicity
N-Methylation
Substrate inhibition
Substrate specificity

ABSTRACT

The *N*-methylation of 4-phenylpyridine produces the neurotoxin 1-methyl-4-phenylpyridinium ion (MPP+). We investigated the kinetics of 4-phenylpyridine *N*-methylation by nicotinamide *N*-methyltransferase (NNMT) and its effect upon 4-phenylpyridine toxicity *in vitro*. Human recombinant NNMT possessed 4-phenylpyridine *N*-methyltransferase activity, with a specific activity of 1.7 ± 0.03 nmol MPP+ produced/h/mg NNMT. Although the K_m for 4-phenylpyridine was similar to that reported for nicotinamide, its k_{cat} of $9.3 \times 10^{-5} \pm 2 \times 10^{-5}\,s^{-1}$ and specificity constant, k_{cat}/K_m, of $0.8 \pm 0.8\,s^{-1}\,M^{-1}$ were less than 0.15% of the respective values for nicotinamide, demonstrating that 4-phenylpyridine is a poor substrate for NNMT. At low (< 2.5 mM) substrate concentration, 4-phenylpyridine *N*-methylation was competitively inhibited by dimethylsulphoxide, with a K_i of 34 ± 8 mM. At high (> 2.5 mM) substrate concentration, enzyme activity followed substrate inhibition kinetics, with a K_i of 4 ± 1 mM. *In silico* molecular docking suggested that 4-phenylpyridine binds to the active site of NNMT in two non-redundant poses, one a substrate binding mode and the other an inhibitory mode. Finally, the expression of NNMT in the SH-SY5Y cell-line had no effect cell death, viability, ATP content or mitochondrial membrane potential. These data demonstrate that 4-phenylpyridine *N*-methylation by NNMT is unlikely to serve as a source of MPP+. The possibility for competitive inhibition by dimethylsulphoxide should be considered in NNMT-based drug discovery studies. The potential for 4-phenylpyridine to bind to the active site in two binding orientations using the same active site residues is a novel mechanism of substrate inhibition.

1. Introduction

Nicotinamide *N*-methyltransferase (NNMT, E.C. 2.1.1.1) *N*-methylates nicotinamide to produce 1-methylnicotinamide using *S*-adenosylmethionine as cofactor (Aksoy et al., 1994). NNMT is a cytosolic enzyme of approximately 29 kDa which is expressed in a variety of tissues, with highest level of expression in the liver (Parsons et al., 2002). NNMT expression in the healthy population follows a bimodal distribution, with 25% of subjects within each of low and high expressor categories (Smith et al., 1998; Parsons et al., 2002, 2003). NNMT has central roles in cellular energy homeostasis, signalling, survival and morphology (Parsons et al., 2011; Williams et al., 2012; Thomas et al., 2013), and in the human naïve embryonic stem cell it has been proposed as one of the main controllers of the epigenetic landscape (Sperber et al., 2015). The enzyme also has been proposed as a therapeutic target for the treatment of many diseases such as cancers

Abbreviations: 4-PP, 4-phenylpyridine; DMSO, dimethylsulphoxide; DV, dependent variable; hNNMT, recombinant human NNMT; IV, independent variable; k_{cat}/K_m, catalytic efficiency; MeNH, 2*N*-methylnorharman; MMP, mitochondrial membrane potential; MPP+, 1-methyl-4-phenylpyridinium ion; MTT, 3-(4,5-dimethylthiazol-2-yl)-2,5-diphenyltetrazolium bromide; NNMT, nicotinamide *N*-methyltransferase; PD, Parkinson's disease

* Corresponding authors.
E-mail addresses: n.i.martin@uu.nl (N.I. Martin), richard.parsons@kcl.ac.uk (R.B. Parsons).
[1] Both of these authors contributed equally to this work.

https://doi.org/10.1016/j.biocel.2018.03.010
Received 27 September 2017; Received in revised form 23 February 2018; Accepted 12 March 2018
Available online 13 March 2018
1357-2725/

(Kim et al., 2009; Emanuelli et al., 2010; Jung et al., 2017).

Early studies upon the substrate specificity of porcine NNMT revealed a number of non-physiological substrates, comprising close structural analogues of nicotinamide, for example thionicotinamide and 3-acetylpyridine (Alston and Abeles, 1988). These studies have been extensively cited in the literature to justify the identification of NNMT as responsible for the *N*-methylation of a range of pyridine-containing compounds such as quinolines and β-carbolines (Parsons et al., 2002, 2003; Williams and Ramsden, 2005). Our recent studies have shown that the majority of these are poor NNMT substrates, with only isoquinoline demonstrating a catalytic efficiency (k_{cat}/K_m) value greater than 30% of that observed for nicotinamide (van Haren et al., 2016; Thomas et al., 2016).

The potential *N*-methylation of these endogenously-available compounds by NNMT is of interest as their *N*-methylated derivatives share close structural similarity to the potent Complex I inhibitor and dopaminergic neurotoxin 1-methyl-4-phenylpyridinium ion (MPP+) (Parsons et al., 2002, 2003; van Haren et al., 2016; Thomas et al., 2016). We have shown that NNMT is expressed in the dopaminergic neurones of the substantia nigra, which are destroyed in Parkinson's disease (PD) (Parsons et al., 2002). Significantly, the enzyme is overexpressed in the cerebellum and caudate nucleus of brains of patients who have died of PD (Parsons et al., 2002, 2003). Thus it has been suggested that *N*-methylation may contribute to PD pathogenesis (Gearhart et al., 2000; Matsubara et al., 2002; Parsons et al., 2002, 2003; Williams and Ramsden, 2005).

4-Phenylpyridine (4-PP) is of interest because its *N*-methylated derivative is MPP+. 4-PP is an exogenously-derived compound found in, amongst others, oranges (Thomas and Bassols, 1992) and mint (Snyder and D'Amato, 1985). 4-PP *N*-methylation by NNMT provides a direct metabolic pathway for the endogenous production of MPP+ (Fig. 1). Due to its small size (155 Da) and hydrophobic nature (predicted logP = 2.6), 4-PP is likely to cross the blood brain barrier. Once inside the brain, its *N*-methylation by NNMT may lead to the accumulation of MPP+ and thus contribute to toxicity.

We have previously reported that 4-PP is a substrate of NNMT, although its kinetics and its effect upon toxicity *in vitro* were not investigated (van Haren et al., 2016). Hence, in this study, we have (1) investigated the kinetics of 4-PP *N*-methylation using recombinant human NNMT (hNNMT), and (2) investigated the effect of NNMT expression upon 4-PP toxicity *in vitro*.

2. Materials and methods

2.1. Materials

Unless otherwise stated, all reagents were purchased from Sigma-Aldrich (Poole, UK) and were of the highest grade available. Cell culture reagents were purchased from Life Technologies (Paisley, UK). 4-PP was purified of contaminating MPP+ using preparative HPLC.

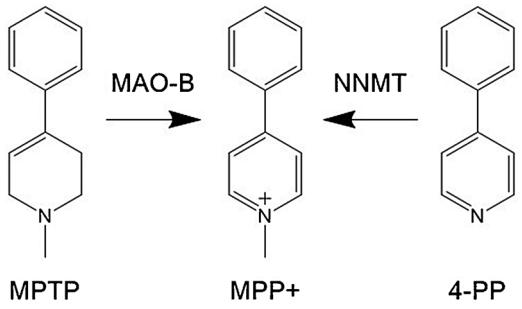

Fig. 1. Biosynthetic routes for 1-methyl-4-phenylpyridinium ion. MPP+ is produced within the brain *via* the monoamine oxidase B-mediated oxidation of MPTP. An alternative route of production has been proposed to occur *via* the NNMT-mediated *N*-methylation of 4-PP.

2.2. 4-Phenylpyridine N-methyltransferase enzyme assay

The ability of NNMT to *N*-methylate 4-PP was assessed using our previously-described NNMT assay (van Haren et al., 2016). hNNMT prepared as previously described (Thomas et al., 2016) was incubated with 1 mM 4-PP prepared in dimethylsulphoxide (DMSO) (5% v/v final concentration, approximately 700 mM) for 32 min. Samples were taken immediately after the addition of 0.5 mM *S*-adenosylmethionine (100 μM final concentration) and subsequently at time points shown in Fig. 2A. MPP+ content was calculated using a MPP+ standard curve and expressed as pmol MPP+ produced ± SD. Linearity of pmol MPP+ produced *vs.* time was determined by linear regression analysis using Prism v5.0 (GraphPad, San Diego, CA, USA). Specific activity was calculated and expressed as pmol MPP+ produced/h/mg hNNMT ± SD ($n = 3$).

2.3. Kinetic analysis

hNNMT was incubated as described in Section 2.2 with 0–10 mM 4-PP. Samples were taken at time points as described above, and initial velocity was calculated and expressed as nmol MPP+ produced/h. Data were modelled initially using Michaelis-Menten non-linear regression analysis. Due to the presence of substrate inhibition, two further analyses were performed as previously described (Patel et al., 2013): (1) non-linear regression analysis using the following substrate inhibition kinetics equations (Lin et al., 2001; Wu, 2011):

$$v = \frac{Vmax.\,[S]}{Km + [S](1 + \frac{[S]}{Ki})} \quad (1)$$

$$v = Vmax.\,\frac{\left(\frac{[S]}{Km}\right) + \left(\frac{\beta[S]^2}{\alpha KmKi}\right)}{1 + \frac{[S]}{Km} + \frac{[S]}{Ki} + \frac{[S]^2}{\alpha KmKi}} \quad (2)$$

and (2) Michaelis-Menten non-linear regression analysis of data from 0 to 1 mM 4-PP, *i.e.* prior to the onset of substrate inhibition at high substrate concentrations and thus representative of kinetics if NNMT were not to undergo substrate inhibition; such an approach has been used by ourselves and others (Lin et al., 2001; Patel et al., 2013; Bomati and Noel, 2005; Han et al., 2017). The kinetic constants K_m, k_{cat} and K_i were calculated for each modelling paradigm and expressed as μM ± SD (K_m and K_i) and s^{-1} ± SD (k_{cat}) ($n = 3$). K_m and k_{cat} were used to calculate k_{cat}/K_m, which was expressed as $s^{-1}M^{-1}$ ± SD ($n = 3$).

2.4. Effect of DMSO concentration upon 4-phenylpyridine N-methylation

Kinetic analysis of 4-PP *N*-methylation was performed as described in Section 2.2, with 4-PP prepared in 1%, 3% and 5% DMSO (v/v final concentrations in reaction samples, approximately 140, 420 and 700 mM respectively). Data were calculated and expressed as nmol 4-PP produced/h ± SD ($n = 3$) and subjected to various analyses as described in Section 3.2.

2.5. Molecular docking of 4-phenylpyridine to the active site of NNMT

Docking of 4-PP into the active site of human NNMT was performed using the Molegro Virtual Docker software (Thomsen and Christensen, 2006), the 2.72 Å resolution X-ray crystal structure of the NNMT enzyme complexed with *S*-adenosyl homocysteine and nicotinamide (Protein Databank entry, 3ROD (Peng et al., 2011), downloaded from the PDBe website http://www.ebi.ac.uk/pdbe (Berman et al., 2016; Young et al., 2017)), and a 3D model of 4-PP downloaded from the NCBI Pubchem website (https://pubchem.ncbi.nlm.nih.gov/) (Kim et al., 2016). The docking of the 4-PP ligand was confined within an 8 Å radius sphere centred on the known nicotinamide binding site, and with the *S*-adenosyl homocysteine retained in its bound position. Following a

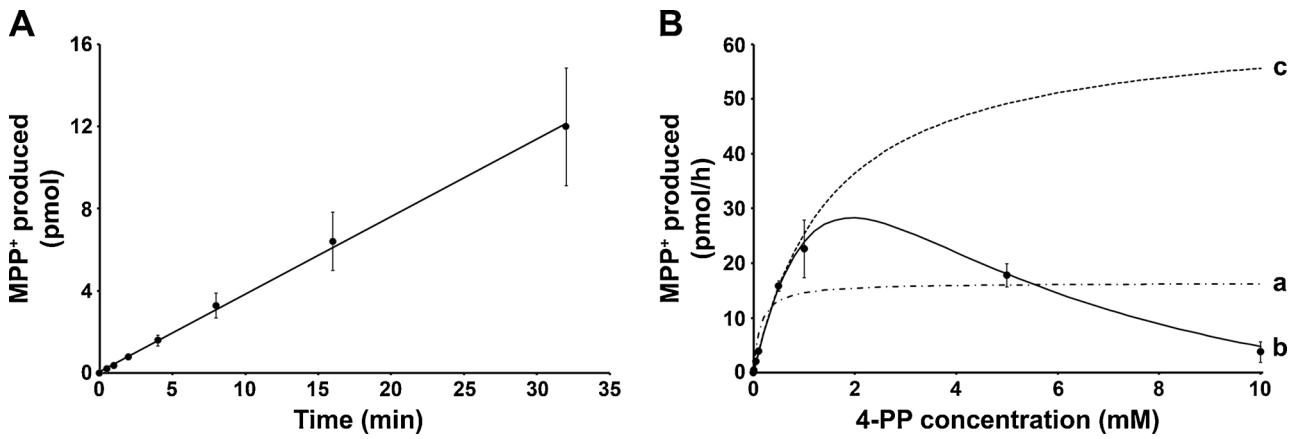

Fig. 2. Kinetic analysis of 4-phenylpyridine *N*-methylation by NNMT. (A) Linearity of MPP+ production with time. Results are expressed as pmol MPP+ produced ± SD (n = 3). (B) Non-linear regression analysis of 4-PP *N*-methylation using various kinetic models to obtain values for V_{max}, K_m and K_i. Results are expressed as pmol MPP+ produced/h ± SD (n = 3). a = Michaelis-Menten kinetics; b = substrate inhibition kinetics using Eq. (2); c = Michaelis-Menten kinetics of data truncated at 1 mM 4-PP.

rigid body docking of the 4-PP, the conformation and position of the ligand were optimised to establish and/or improve hydrogen bonding to the protein.

2.6. Cell culture

SH-SY5Y human neuroblastoma cells (which have no endogenous NNMT expression) and S.NNMT.LP cells (comprising SH-SY5Y stably expressing a recombinant NNMT C-terminally fused with the V5 epitope) were cultured as previously described (Parsons et al., 2011; Thomas et al., 2013, 2016). NNMT protein and mRNA expression were confirmed using Western blotting and RT-PCR respectively (Parsons et al., 2011) (data not shown).

2.7. 3-(4,5-Dimethylthiazol-2-yl)-2,5-diphenyltetrazolium bromide reduction assay

Cells were seeded at a density of 15,000 cells/well into the wells of a 96-well plate (Thermo Scientific, Loughborough, UK) in quadruplicate and incubated with 4-PP (12.5–1600 μM) for 48 and 120 h. As a positive control, cells were incubated with 500 μM 2*N*-methylnorharman (MeNH). Cell viability was assessed using the 3-(4,5-dimethylthiazol-2-yl)-2,5-diphenyltetrazolium bromide (MTT) reduction assay as previously described (Thomas et al., 2015). Results were calculated and expressed as percentage cell viability compared with that of untreated cells ± SD (n = 3 for 48 h, n = 5 for 120 h). Concentration was log-transformed and subsequently data were modelled using non-linear regression analysis using the following equation:

$$y = minimum + \frac{maximum - minimum}{1 + 10^{(LogEC50 - x)*hillslope}} \quad (3)$$

with a constraint of y = 0 for the minimum. From this, $logEC_{50}$ was calculated for each replicate from which an average $logEC_{50}$ ± SD (n = 3 for 48 h, n = 5 for 120 h) was calculated. To aid comprehension, this $logEC_{50}$ value was antilogged to obtain EC_{50}, which was expressed as μM; SD values were not antilogged due to the asymmetry obtained when the antilog of a logSD is obtained (Hancock et al., 1988).

2.8. Lactate dehydrogenase cell death assay

Cells were seeded and incubated with 4-PP as outlined in Section 2.7 for 120 h, after which cell death was measured using the Pierce LDH Cytotoxicity Assay Kit (Thermo Fisher Scientific, Paisley, UK) as previously described (Thomas et al., 2015). Results were calculated, expressed and modelled using non-linear regression as described in Section 2.7, with a constraint of y = 0 for the maximum (n = 4).

2.9. Cellular ATP content assay

Cells were seeded as described in Section 2.7 into the wells of a poly-*L*-lysine-coated white 96-well plate (Greiner Bio-One Ltd., Stonehouse, UK) and incubated with 4-PP as described in Section 2.7 for 120 h. ATP content was measured as previously described (Thomas et al., 2016) and expressed as percentage cellular ATP content compared with that of untreated cells ± SD (n = 5). Non-linear regression analysis was performed as described in Section 2.7.

2.10. Mitochondrial membrane potential

Cells were seeded as described in Section 2.7 into the wells of a poly-*L*-lysine-coated black 96-well plate (Thermo Scientific, Loughborough, UK) and incubated with MPP+ as described in Section 2.7 for 120 h. Membrane mitochondrial potential (MMP) was measured using the JC-1 mitochondrial membrane potential assay kit (Cayman Chemical Company, Michigan, USA) as previously described (Parsons et al., 2011) and expressed as percentage observed in untreated cells ± SD (n = 4). Non-linear regression analysis was performed as described in Section 2.7.

2.11. Statistical analysis

All analyses were undertaken using Prism v5.0. In all instances, $P < 0.05$ was taken to indicate statistical significance. Statistical analysis of cell viability, cell death, cellular ATP content and MMP was performed as previously described (Thomas et al., 2016). Briefly, comparison of all four endpoint measures at each concentration with values observed in untreated cells was performed using one-way ANOVA with Tukey *post-hoc* comparisons, with concentration as independent variable (IV) and endpoint measure as dependent variable (DV). Comparison of toxicity between cell lines and time points for each concentration was performed using two-way ANOVA with Dunnett's *post-hoc* comparisons, with cell line and 4-PP or MeNH concentration as IV and endpoint measure as DV. Statistical comparison of EC_{50}s obtained from the MTT reduction assay was performed using two-way ANOVA, with cell line and length of incubation as IVs and $logEC_{50}$ as DV. Statistical comparison of cell death, cellular ATP content and MMP EC_{50} values were performed using Student's *t*-test with Welch correction, with cell line as IV and $logEC_{50}$ as DV. Statistical comparisons were performed upon $logEC_{50}$ values as they follow a normal distribution (Hancock et al., 1988).

Table 1
Calculated K_m, K_i, k_{cat} and k_{cat}/K_m values for NNMT 4-phenylpyridine *N*-methyltransferase activity. Values are expressed ± SD.

Non-linear regression analysis	K_m (μM)	K_i (μM)	$k_{cat} \times 10^{-4}$ (s^{-1})	K_{cat}/K_m ($s^{-1} M^{-1}$)
Michaelis-Menten	125 ± 111	–	0.93 ± 0.2	0.8 ± 0.8
Substrate inhibition[a]	2375 ± 187	4011 ± 963	5.7 ± 0.3	0.2 ± 0.03
Truncated Michaelis-Menten[b]	1511 ± 348	–	3.6 ± 0.5	0.2 ± 0.09
Nicotinamide[c]	199 ± 32	–	1000	510

[a] Calculated using Eq. (2) outlined in Section 2.2.
[b] Data was truncated to include only 0–1 mM 4-PP.
[c] Data previously calculated for nicotinamide shown for comparison purposes.

3. Results

3.1. NNMT demonstrated 4-phenylpyridine N-methyltransferase activity and substrate inhibition kinetics

To determine whether NNMT was capable of *N*-methylating 4-PP, we incubated hNNMT with 1 mM 4-PP prepared in DMSO (5% v/v final concentration, approximately 700 mM) (Fig. 2). MPP+ production increased linearly with time (Fig. 2A), with a specific activity of 1.7 ± 0.03 nmol MPP+ produced/h/mg hNNMT.

To estimate kinetic constants for 4-PP *N*-methylation, we incubated NNMT with 4-PP (0–10 mM), and performed Michaelis-Menten non-linear regression analysis upon resulting initial velocities (Fig. 2B). The results are summarised in Table 1. Comparison with values published for nicotinamide (van Haren et al., 2016) revealed that 4-PP is a poor substrate for NNMT. Michaelis-Menten analysis produced a K_m similar to that we have previously reported for nicotinamide, whereas k_{cat} and k_{cat}/K_m were only 0.1% and 0.15% of those for nicotinamide. Due to the poor goodness of fit obtained ($R^2 = 0.54$), the data was subsequently modelled using non-linear substrate inhibition kinetics which, although providing significantly better goodness of fit ($R^2 = 0.96$), returned ambiguous values for Vmax, K_m and K_i (data not shown). Data was then modelled with a variety of substrate inhibition equations in order to obtain a best kinetic fit (Lin et al., 2001; Wu, 2011). K_m was 12-fold higher than that reported for nicotinamide, with k_{cat} and k_{cat}/K_m being 0.6% and 0.04% of the respective values. The k_i for 4-PP substrate inhibition was similar to those reported for other NNMT substrates which demonstrated substrate inhibition, which were in the range 4.7–20.2 mM (van Haren et al., 2016). To estimate kinetic parameters for 4-PP *N*-methylation in the absence of substrate inhibition, data between 0–1 mM 4-PP, *i.e.* prior to the onset of substrate inhibition, were subjected to Michaelis-Menten analysis ($R^2 = 0.96$). The resulting K_m was 8-fold higher, and k_{cat} and k_{cat}/K_m values were 0.4 and 0.04%, of values for nicotinamide.

3.2. DMSO is a competitive inhibitor of 4-phenylpyridine N-methylation by NNMT

As DMSO is reported to be a competitive inhibitor of a number of enzymes (Plummer et al., 1983; Banasik et al., 2004; Kwak et al., 2009), we investigated whether DMSO was a competitive inhibitor of 4-PP *N*-methylation by NNMT (Fig. 3).

Specific activity decreased with increasing DMSO concentration (Fig. 3A), resulting in specific activities of 2.6 ± 0.06, 1.8 ± 0.05 and 1.5 ± 0.1 nmol MPP+ produced/h/mg hNNMT at 1, 3 and 5% DMSO (v/v final concentration) respectively ($P < 0.001$). Non-linear substrate inhibition regression analysis of the data (Fig. 3B) revealed that increasing DMSO concentration decreased velocity, *v*, at 4-PP concentrations below 2.5 mM, *i.e.* prior to the onset of substrate inhibition. As it is likely that physiological concentrations of 4-PP are below 2.5 mM, Michaelis-Menten kinetic modelling was performed using data truncated at 2.5 mM (Fig. 3C), from which apparent K_m (K_m^{app}) and V_{max} (V_{max}^{app}) values for each concentration of DMSO were calculated, which are summarised in Table 2. V_{max}^{app} values did not alter significantly whereas K_m^{app} values increased with increasing DMSO concentration, hence DMSO is a competitive inhibitor of 4-PP *N*-methylation. As a confirmatory exercise, the same data were modelled using an Eadie-Hofstee plot, *v vs. v*/[S] (Fig. 3D), which confirmed the presence of competitive inhibition of 4-PP *N*-methylation by DMSO. The k_{cat} and k_{cat}/K_m values for all concentrations of DMSO were calculated and are summarised in Table 2. As expected for a competitive inhibitor, k_{cat} did not alter whereas k_{cat}/K_m decreased with increasing DMSO concentration. Catalytic efficiency was significantly reduced by all three concentrations of DMSO, with an 82% reduction at 1% v/v DMSO.

To estimate the K_m of 4-PP in the absence of DMSO, K_m^{app} was plotted against DMSO concentration (Plummer et al., 1983) (Fig. 3E), from which K_m was calculated *via* extrapolation as 155 μM. The K_i for DMSO substrate inhibition was calculated by first calculating the inhibition factor, α, for each concentration of DMSO using the following equation:

$$\alpha Km = Km^{app}$$

K_i was then calculated using the following equation:

$$\alpha = 1 + \frac{[\mathrm{DMSO}]}{K_i}$$

All three K_i values were then averaged to obtain a mean of 34 ± 8 mM.

K_m and V_{max} values of 155 μM and 48 pmol MPP+ produced/h (V_{max} being derived from the average of V_{max}^{app} for all three concentrations of DMSO) were then used to calculate the activity of 4-PP *N*-methylation in the absence of DMSO using Michaelis-Menten regression analysis (Fig. 3C). Specific activity in the absence of DMSO was extrapolated from a plot of specific activity *vs.* DMSO concentration (Fig. 3F), from which the specific activity was estimated to be 2.8 ± 0.2 nmol MPP+ produced/h/mg hNNMT.

3.3. 4-Phenylpyridine docks to the hNNMT active site in two non-redundant orientations

Molecular docking was used to investigate the interaction of 4-PP with the NNMT active site. To confirm the accuracy of the docking protocol, initially hNNMT was docked with nicotinamide (Fig. 4A). As expected (Peng et al., 2011), the pyridine ring of nicotinamide formed an electrostatic interaction with Y20 and was also held within a hydrophobic clamp comprising Y204 and L164. The amide group of nicotinamide formed hydrogen bonds with S201, S213 and D197.

A total of 50 docking trials for 4-PP were made, yielding just two non-redundant 4-PP poses (taking an RMSD ≤ 1 Å on atomic co-ordinates as the criterion of pose similarity), each of which was returned 25 times. The first pose presented 4-PP in a presumed substrate binding mode (Fig. 4B), in which the 4-PP pyridine ring interacted with Y20, Y204 and L164 as described for nicotinamide. However, due to the lack of an amide group, there were no hydrogen bonding interactions between 4-PP and S201, S213 and D197. There were no interactions between the aromatic phenyl ring of 4-PP and the active site of hNNMT.

In the second pose, 4-PP was orientated almost 180° with respect to the first pose (Fig. 4C). This second pose most likely represents an inhibitory binding mode due to the lack of proximity between the pyridine nitrogen and the catalytically essential Y20 (Peng et al., 2011). The phenyl ring formed a hydrophobic interaction with L164 and pi-pi stacking with Y204. The pyridine nitrogen of 4-PP is orientated in a similar position to the amide nitrogen of nicotinamide, hence forming hydrogen bond interactions with S201 and S213, but not D197.

Docking studies were also performed using isoquinoline (Fig. 5), a

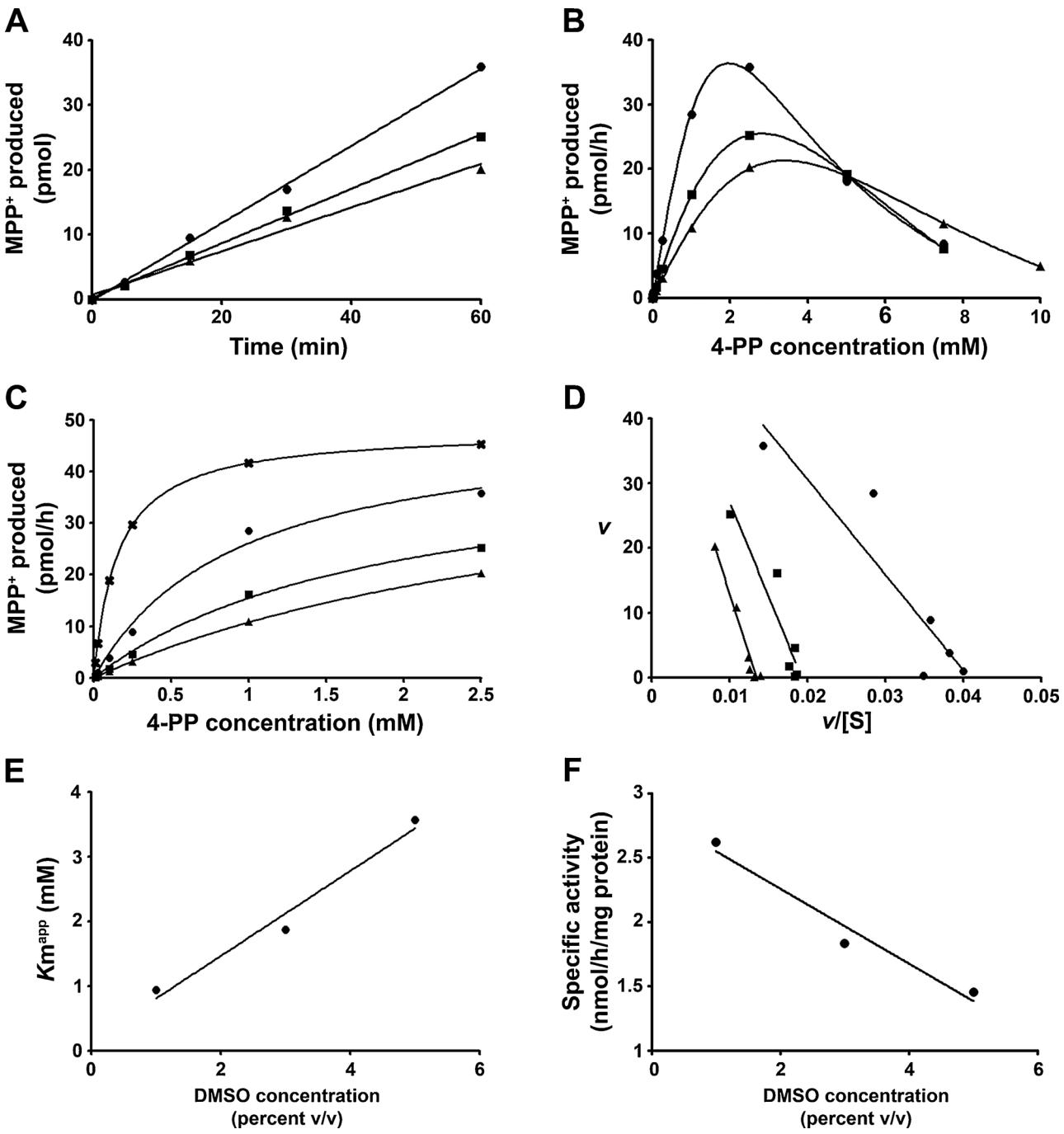

Fig. 3. Analysis of the effect of dimethylsulphoxide upon 4-phenylpyridine *N*-methylation kinetics. (A) Effect of increasing DMSO concentration upon linearity of MPP+ production with time. (B) Non-linear substrate inhibition kinetic regression analysis of the effect of increasing DMSO concentration upon MPP+ production. (C) Michaelis-Menten kinetic modelling of data truncated at 2.5 mM 4-PP, which was subsequently used to obtain K_m and V_{max} values for each concentration of DMSO. For comparison, kinetic analysis of enzyme activity in the absence of DMSO, predicted using V_{max} and K_m values calculated from data presented in this and panel E, is also shown. (D) Eadie-Hofstee plot of data truncated at 2.5 mM 4-PP, confirming the presence of competitive inhibition of 4-PP *N*-methylation by DMSO. (E) Effect of DMSO concentration upon apparent K_m, calculated using data presented in panel C, from which an estimate for K_m in the absence of DMSO was obtained *via* extrapolation. (F) Effect of DMSO concentration upon specific activity, from which an estimate for specific activity in the absence of DMSO was obtained *via* extrapolation. For panels A–D: ● = 1% DMSO; ■ = 3% DMSO; ▲ = 5% DMSO. For panel D only: × = predicted activity in the absence of DMSO. All concentrations of DMSO are v/v.

substrate of NNMT which also demonstrates substrate inhibition (van Haren et al., 2016). As observed with 4-PP, a total of 50 docking trials yielded just two non-redundant poses, each of which was returned 25 times. The first pose presented isoquinoline in a presumed substrate binding mode (Fig. 5A) and the second a presumed inhibitory binding mode (Fig. 5B), as determined by the relative proximity of the pyridine nitrogen to Y20. Each pose used the same active site residue interactions with the phenyl and pyridine rings as observed for 4-PP.

3.4. Neither NNMT expression nor length of incubation influenced 4-phenylpyridine toxicity in vitro

The MTT reduction cell viability assay, an early-stage measure of toxicity (Thomas et al., 2015), was used to determine whether NNMT increased 4-PP toxicity *in vitro* after 48 and 120 h incubation (Fig. 6 and Tables 3 and 4). 4-PP was toxic towards both SH-SY5Y and S.NNMT.LP cells at concentrations of 400, 800 and 1600 μM at both time points

Table 2
Calculated values of K_{mapp}, k_{cat} and k_{cat}/K_m for dimethylsulphoxide competitive inhibition.

DMSO (% v/v)	V_{max}^{app} (pmols MPP+/h)	K_m^{app} (μM)	$k_{cat} \times 10^{-4}$ (s^{-1})	k_{cat}/K_m ($s^{-1} M^{-1}$)	Catalytic efficiency (percentage)[a]
0[b]	48.1	155	2.8	1.7	100
1	51	939	2.8	0.3	18
3	44	1869	2.5	0.1	6
5	49	3565	2.8	0.08	5

[a] Catalytic efficiency expressed as percentage of k_{cat}/K_m at 0% DMSO.
[b] Predicted values, calculated as described in Section 3.2.

(Table 3). The length of incubation had no effect upon 4-PP toxicity at any of the concentrations investigated for either cell-line. There was no significant difference in $logEC_{50}$ for each cell-line at either time point (Table 4). As a positive control for the effect of NNMT expression upon toxicity, the effect of 0.5 mM MeNH, a compound whose *in vitro* toxicity we have shown to increase with length of incubation, was investigated. MeNH was significantly more toxic towards both SH-SY5Y and S.NNMT.LP cells after 120 h compared with 48 hr incubation (SH-SY5Y: 78.5 ± 3% *vs.* 10.7 ± 6.1%, $P < 0.001$, $n = 3$; S.NNMT.LP: 52.2 ± 3.8% *vs.* 22.1 ± 18.4%, $P < 0.01$, $n = 4$). MeNH was significantly more toxic towards S.NNMT.LP compared to SH-SY5Y cells after 48 h incubation ($P < 0.05$), although after 120 h incubation there was no difference in toxicity.

The LDH cytotoxicity assay, a late-stage measure of toxicity (Thomas et al., 2015), was used as an additional confirmatory toxicity assay (Fig. 7A and Table 3). 4-PP was toxic towards SH-SY5Y cells at 1600 and 800 μM, and towards S.NNMT.LP cells at 1600, 800 and 400 μM. There was no significant difference in $logEC_{50}$ values for each cell-line (−2.51 ± 0.3 *vs.* −2.17 ± 0.1, equivalent to 3090 μM and 6761 μM respectively, $P = 0.2$).

The low catalytic efficiency of 4-PP *N*-methylation by NNMT (Table 2) in tandem with the lack of effect of NNMT expression upon 4-PP toxicity *in vitro* suggested that the degree of intracellular 4-PP *N*-methylation by NNMT was insignificant. As a confirmatory exercise, we investigated the effect of NNMT expression after 120 h incubation upon two parameters of mitochondrial function – cellular ATP content and MMP (Parsons et al., 2011). Our hypothesis was that increased 4-PP *N*-methylation by NNMT would result in increased MPP+ production and accumulation within the cell, the consequence of which would be Complex I inhibition, a decrease in the MMP (Fig. 7B and Table 3) and a subsequent reduction in intracellular ATP content (Fig. 7C and Table 3). The MMP of SH-SY5Y cells was significantly decreased at 200, 400, 800 and 1600 μM 4-PP, and in S.NNMT.LP cells at 400, 800 and 1600 μM 4-PP. There was no significant difference in MMP between each cell-line at any concentration of 4-PP investigated. There was no significant difference in $logEC_{50}$ for each cell-line (−2.69 ± 0.32 *vs.* −2.17 ± 0.14, equivalent to 2023 *vs.* 2280 μM, $P = 0.5$).

Intracellular ATP content of SH-SY5Y cells was significantly decreased at 800 and 1600 μM 4-PP, yet was increased at 100, 200 and 400 μM. In S.NNMT.LP cells, 4-PP decreased intracellular ATP content at concentrations of 800 and 1600 μM, with no concentration increasing intracellular ATP concentration. Intracellular ATP content was significantly higher in SH-SY5Y cells compared with that of S.NNMT.LP cells at 200 (157.6 ± 19.7% *vs.* 109.8 ± 34.4%, $P < 0.01$) and 400 μM (135.2 ± 23% *vs.* 95.2 ± 25.9%, $P < 0.05$) 4-PP. There was no significant difference in $logEC_{50}$ values for each cell-line (−3.13 ± 0.04 *vs.* −3.2 ± 0.07, equivalent to 738 *vs.* 625 μM, $P = 0.12$).

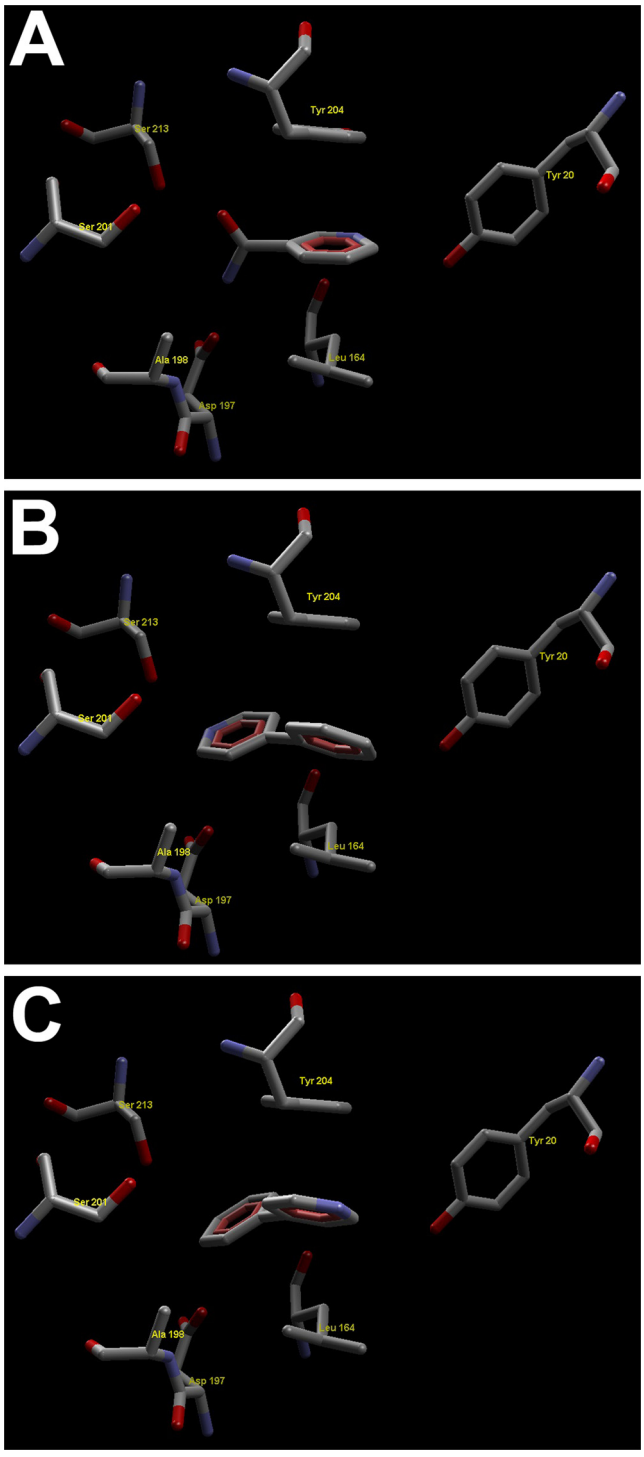

Fig. 4. *In silico* molecular docking of nicotinamide and 4-phenylpyridine to the active site of NNMT. (A) Nicotinamide. (B) 4-PP in a predicted substrate binding orientation. (C) 4-PP in a predicted inhibitor binding orientation.

4. Discussion

4.1. 4-PP is a substrate of NNMT

Our kinetic analysis of 4-PP *N*-methylation by hNNMT demonstrated that 4-PP was rather a poor substrate, even when the inhibitory effect of DMSO was taken into account. 4-PP is an exogenous compound whose abundance in the diet is very low. Its content in *Brassica campestris* L. ssp. *Pekinensis*, for example, is as little as 0.9% (Hong and Kim,

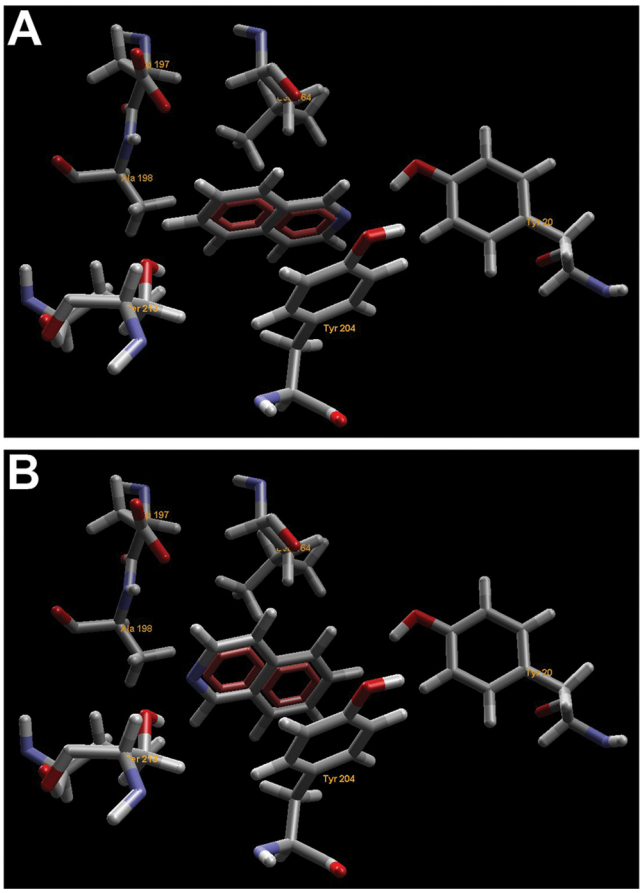

Fig. 5. *In silico* molecular docking of isoquinoline to the active site of NNMT. (A) Isoquinoline in a predicted substrate binding orientation. (B) Isoquinoline in a predicted inhibitor binding orientation.

2013). Hence, even for someone eating an exclusively vegetarian diet it is unlikely that the concentration of 4-PP within the brain will be sufficiently high to outcompete nicotinamide as a substrate for NNMT. Even if it were to reach such a concentration, the low rate of catalytic turnover would more likely result in the inhibition of nicotinamide *N*-methylation. Hence, it is unlikely that NNMT-mediated 4-PP metabolism is a source of MPP+. This is supported by the failure of NNMT expression to increase the toxicity of 4-PP due to increased MPP+ production in S.NNMT.LP cells, even at concentrations which were significantly higher than what would be expected physiologically. As MPP+ is actively sequestered into mitochondria due to its positive charge (Trevor et al., 1987), it could be argued that, with even such a low catalytic turnover, over a much longer period of time the slow but continuous *N*-methylation of 4-PP may result in a toxic accumulation of MPP+ within the mitochondria, resulting in Complex I inhibition and depletion of the MMP, and ultimately cell death. It is also possible that mature neurones, which rely predominantly upon mitochondrially-derived ATP (Zheng et al., 2016), may be more susceptible to long-term MPP+ accumulation, compared to tumour cells in culture which rely predominantly upon glycolysis (Vander Heiden et al., 2009). *In vivo* studies using acute high-dose 4-PP administration have failed to support this (Bradbury et al., 1985; Perry et al., 1987; Irwin et al., 1987; Godin and Crooks, 1989; Carr and Basham, 1991) and to date no study using NNMT-overexpressing *in vivo* models have reported such observations.

4.2. 4-PP N-methylation by NNMT displayed substrate inhibition kinetics

Although 4-PP is a minor substrate of NNMT, its kinetics are of interest as they reveal that NNMT-mediated 4-PP *N*-methylation was subject to both substrate and competitive inhibition. Below concentrations of 2.5 mM 4-PP, competitive inhibition by DMSO was observed, whereas at concentrations higher than 2.5 mM, substrate inhibition occurred. This has important consequences for NNMT-based drug discovery studies, as it is a therapeutic target for a number of diseases, in particular cancer.

Molecular docking revealed that 4-PP is able to dock with the NNMT active site in two non-redundant poses, one of which we propose is a substrate binding mode and the other an inhibitory binding mode as deduced by the proximity of the pyridine nitrogen to Y20. The substrate inhibition can thus be rationalised to arise due to competition between these two binding modes. In its inhibitory binding mode, 4-PP interacts with the active site *via* both its phenyl and pyridine rings, whereas in its substrate binding mode it interacts only *via* its pyridine ring, with the increased number of interactions presumably favouring the inhibitory binding mode at high 4-PP concentration.

Mechanistically, this is of interest, as it represents a previously unreported mechanism of substrate inhibition. To date, two mechanistic models have been proposed. The first model involves the formation of a ternary dead-end complex comprising the substrate interacting with the end-product of cofactor metabolism within the active site at high substrate concentrations (Wu, 2011; Tyapochkin et al., 2009). The second model predicts the presence of two substrate binding sites, the first a catalytically-active high affinity site and the second a

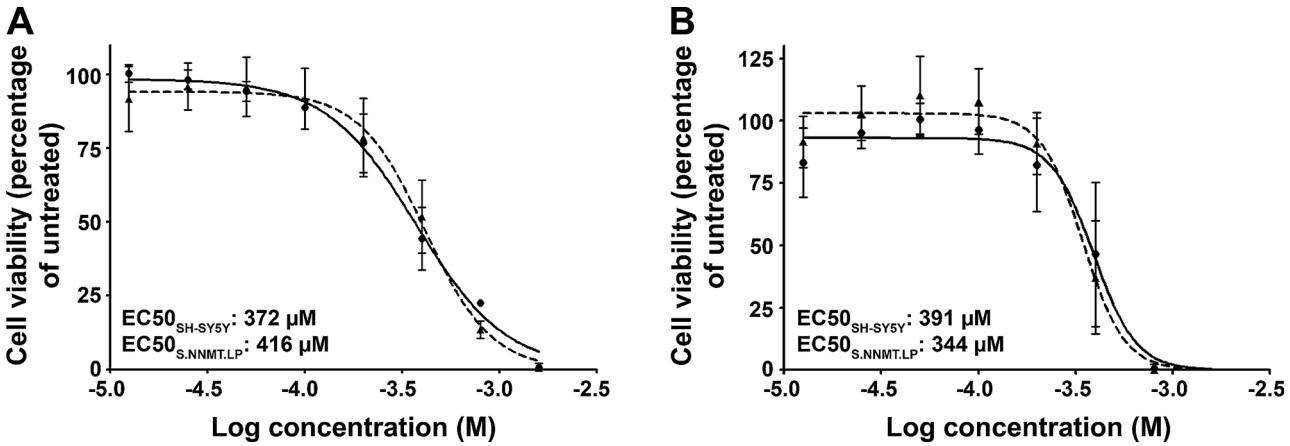

Fig. 6. Effect of NNMT expression upon 4-phenylpyridine toxicity *in vitro* using the MTT reduction cell viability assay. Cell viability is expressed as percentage of untreated cells ± SD (n = 3 for 48 h incubation, n = 5 for 120 h incubation). Statistical analysis comprised (i) toxicity of each concentration *vs* untreated cells using one-way ANOVA (results are summarised in Table 3) and (ii) toxicity between cell-lines at each individual concentration using two-way ANOVA (results shown on graph; all comparisons were $P > 0.05$). EC_{50} values shown are derived from $logEC_{50}$ ± SD values. (A) 48 h incubation. (B) 120 h incubation. For both panels: ● = SH-SY5Y; ▲ = S.NNMT.LP.

Table 3
Summary of significant changes in cell viability (MTT) and intracellular ATP concentrations (ATP) in SH-SY5Y and S.NNMT.LP cells. For MTT experiments, results are expressed as percentage viability compared to untreated cells ± SD (n = 3 for 48 h incubation, n = 5 h for 120 h incubation). For LDH experiments, results are expressed as cell death compared to untreated cells ± SD (n = 4). For MMP experiments, results are expressed as percentage observed in untreated cells ± SD (n = 4). For ATP experiments, results are expressed as percentage observed in untreated cells ± SD (n = 5). Statistical analysis comprised comparison of cellular response at each 4-PP concentration compared to untreated cells using one-way ANOVA.

		Concentration (μM)[a]				
		100	200	400	800	1600
MTT 48 h	*SH-SY5Y*	–	–	44.3[b] ± 10.7	22.4 ± 0.7	0.8 ± 1.2
	S.NNMT.LP	–	–	51.8 ± 12.5	13.5 ± 2.9	0.5 ± 0.3
MTT 120 h	*SH-SY5Y*	–	–	46.5 ± 28.8	0.7 ± 1.8	−0.9 ± 0.2
	S.NNMT.LP	–	–	37.2 ± 22.6	0.2 ± 1.3	−1 ± 0.4
LDH	*SH-SY5Y*	–	–	–	22.6 ± 6.7	26.9 ± 5
	S.NNMT.LP	–	–	9.4 ± 3.6**	22 ± 5.2	25 ± 2.3
MMP	*SH-SY5Y*	–	83.5 ± 8.1**	79.3 ± 3.5	70.6 ± 4.6	53.9 ± 1.07
	S.NNMT.LP	–	–	68.7 ± 10.9	65.1 ± 10.9	52.9 ± 7.1
ATP[c]	*SH-SY5Y*	137.4 ± 18.8*	157.6 ± 19.7**	135.2 ± 23*	37.8 ± 15.4**	−1.3 ± 5.1
	S.NNMT.LP	–	–	–	24.4 ± 11.4	−3.1 ± 8.7

[a] Concentrations below 100 μM elicited no significant changes in any of the endpoints measured and are thus not included. The exception to this was a significant decrease in SH-SY5Y cell death at 25 μM 4-PP ($P < 0.05$).
[b] Only statistically significant results are shown and are $P < 0.001$ unless otherwise indicated: * = $P < 0.05$, ** = $P < 0.01$.
[c] ATP content in untreated cells: SH-SY5Y = 178 ± 68 pmol/mg protein; S.NNMT.LP = 337 ± 65 pmol/mg protein.

Table 4
Summary of logEC_{50} ± SD and their corresponding antilog values for the MTT assay. LogEC_{50} values are log Molar concentrations. The antilogs of the EC_{50} values are shown in brackets and are expressed as μM; the antilog of the SD is not shown due to the resulting asymmetry generated. Values are the average of three (48 h) or five (120 h) experiments. Statistical analysis was performed upon the logEC_{50} ± SD values using two-way ANOVA. All comparisons were $P > 0.05$.

	48 h	120 h
SH-SY5Y	−3.43 ± 0.05 (372)	−3.41 ± 0.07 (391)
S.NNMT.LP	−3.38 ± 0.05 (416)	−3.46 ± 0.07 (344)

catalytically-inactive low affinity site, either within or separate to the active site itself (Lin et al., 2001; Wu, 2011). At high substrate concentration, binding to the catalytically-inactive site prevents the binding of substrate to the catalytically-active site either *via* direct steric hindrance, as for example warfarin binding within the active site of cytochrome P450 2C9 (Williams et al., 2003), or the induction of a conformational change of the protein, as for example dehydroepiandrosterone binding to sulphotransferase 2A1 (Tracy and Hummel, 2004; Allali-Hassani et al., 2007). Our molecular docking study suggests a novel mechanism in which 4-PP binds to the active site of NNMT in two orientations, one a catalytic and the other a non-catalytic orientation, both of which bind to a single binding site using the same amino residue interactions. The ability to bind in this manner arises due to 4-PP possessing 2-fold rotational symmetry. In support of this, the majority of NNMT substrates which demonstrate substrate inhibition are quinoline and its analogues, compounds which also demonstrate two-fold rotational symmetry (Fig. 8) and have K_i values similar to that of 4-PP (van Haren et al., 2016). Molecular docking of isoquinoline returned the same binding poses and active site amino acid residue interactions as 4-PP, and has a K_i of 20 mM which is similar to that for

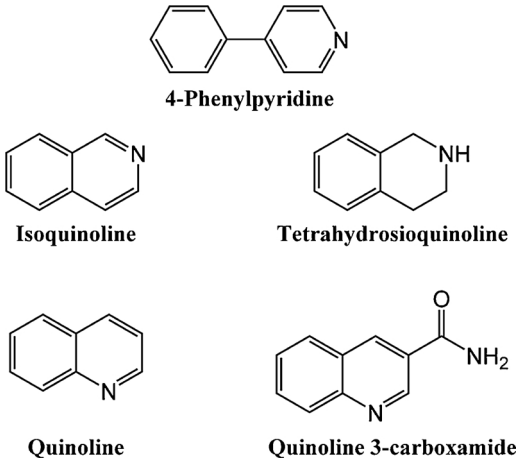

Fig. 8. Structural similarity between 4-phenylpyridine and quinolone analogues whose *N*-methylation by NNMT demonstrate substrate inhibition kinetics.

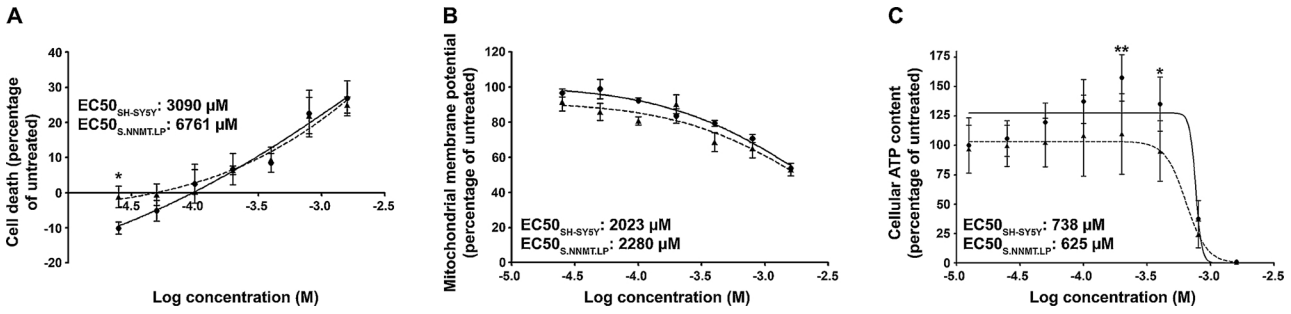

Fig. 7. Effect of NNMT expression upon 4-phenylpyridine toxicity *in vitro* using the LDH cytotoxicity assay, MMP analysis and cellular ATP content assay. (A) Cell death is expressed as percentage observed in untreated cells ± SD (n = 4). (B) MMP is expressed as percentage observed in untreated cells ± SD (n = 4). (C) Cellular ATP content is expressed as percentage observed in untreated cells ± SD (n = 5). For all panels, statistical analysis comprised (i) toxicity of each concentration *vs* untreated cells using one-way ANOVA (results are summarised in Table 3) and (ii) toxicity between cell-lines at each individual concentration using two-way ANOVA (results shown on graph): * = $P < 0.05$; ** = $P < 0.01$. ● = SH-SY5Y; ▲ = S.NNMT.LP.

4-PP.

4.3. 4-PP N-methylation undergoes competitive inhibition by DMSO

Our results demonstrate that DMSO is a competitive inhibitor of 4-PP *N*-methylation by NNMT. Many studies of enzyme kinetic reactions utilise DMSO as a solvent for solubilising non-polar substrates (van Haren et al., 2016; Faulds et al., 2011; Patel et al., 2013), usually at concentrations below 5% (approximately 700 mM). We have shown that preparing nicotinamide in 5% DMSO results in more reliable estimation of the kinetic parameters of nicotinamide *N*-methylation compared to nicotinamide prepared in phosphate-buffered saline, which we ascribed to the relative insolubility of nicotinamide in phosphate-buffered saline compared to DMSO which resulted in less nicotinamide delivered to the assay (Patel et al., 2013). Although DMSO has no effect upon the activity of a number of enzymes (Chauret et al., 1998; Tsitsanou et al., 1999; Easterbrook et al., 2001), DMSO is known to be a competitive inhibitor of many enzymes (Perlman and Wolff, 1968; Plummer et al., 1983; Chauret et al., 1998; Banasik and Ueda, 1999; Easterbrook et al., 2001; Banasik et al., 2004). We were unable to determine, using molecular docking, how DMSO binds to the NNMT active site. This was due to the small size of the molecule and the vast number of potential interactions within the large active site of NNMT. Where crystal structures of DMSO complexed with other enzymes have been obtained, in many instances DMSO interacts with inorganic metal ions within their active sites. For example, the crystal structure of P450 BM-3 reveals that the sulphur atom of DMSO interacts with the iron of the heme group (Kuper et al., 2007). DMSO can also interact directly with amino acid residues. For example, the inhibition of liver alcohol dehydrogenase involves co-ordination with amino acid residue S48 as well as the metal ion within the active site (Meijers et al., 2007). As NNMT does not require an active site metal ion for activity, it can be assumed that DMSO interacts directly with residues within the active site.

The limited numbers of studies which have calculated a K_i for DMSO reveal it to be a poor inhibitor, with values ranging from 5 mM for alcohol dehydrogenase (Perlman and Wolff, 1968) to 70 mM for acetylcholinesterase (Plummer et al., 1983). The K_i for NNMT *N*-methylation of 4-PP is in accord with these values. Although not a potent inhibitor, the concentrations of DMSO routinely used in enzyme reactions are significantly above these K_i values, being approximately 20-fold higher for 4-PP *N*-methylation by NNMT. Therefore it is likely that many studies are performed using sub-optimal enzyme activity, and are thus reporting incorrect K_m and k_{cat}/K_m values, as evidenced in our study. Hence, the use of alternative solvents for kinetic studies such as acetonitrile and methanol should be considered. Studies of cytochrome P450s, UDP glucuronosyltransferases and phenolsulphotransferases show that concentrations of up to 1% methanol and 2% acetonitrile had little effect upon their activities, in contrast to DMSO (Chauret et al., 1998; Easterbrook et al., 2001). However, these solvents can also act as enzyme inhibitors (Busby et al., 1999), so care must be taken to assess the effect of solvents upon enzyme catalytic activity in order to choose the most appropriate.

This is of particular importance for the screening of compounds in drug discovery studies in which the therapeutic target is NNMT. It is possible that, in addition to acting as a competitive inhibitor of substrate metabolism, DMSO may also compete with competitive inhibitors for the active site, thus reducing their efficacy. For example, DMSO binds to the same binding site in the active site of lysozyme as its inhibitor *N*-acetylglucosamine, reducing its inhibitory efficacy (Johannesson et al., 1997). Also, increasing concentrations of DMSO increased the IC_{50} values of all lipophilic and hydrophilic inhibitors of poly(ADP-ribose) synthetase investigated by upto 10-fold, with the IC_{50} of 6(5*H*)-phenanthridinone increasing 33-fold (Banasik and Ueda, 1999). Thus, the use of DMSO in enzyme assays can potentially affect candidate inhibitor efficacy sufficiently to lead to their unwarranted removal from drug inhibitor screens. The small size of DMSO makes its docking to protein active sites somewhat complicated to predict, in particular for enzymes such as NNMT which have large active sites, thus it is very difficult to predict whether DMSO may interfere with candidate inhibitor docking and thus inhibitory activity. However, by using the kinetic approaches used in this study, it will be possible to determine whether DMSO is an appropriate solvent for inhibitor screening, thus reducing the likelihood of removing candidate inhibitors due to incorrect determination of IC_{50} and K_i.

5. Conclusions

These findings suggest that the *N*-methylation of 4-PP into the dopaminergic neurotoxin MPP+ is unlikely to occur within the cell and is thus unlikely to contribute to the pathogenic process of PD.

Conflict of interest

None.

Acknowledgements

MGT was supported by a King's College London Graduate Schools Studentship. The funding body had no involvement in study design, collection, analysis or interpretation of data, writing the report or the decision to submit.

References

Aksoy, S., Szumlanski, C.L., Weinshilboum, R.M., 1994. Human liver nicotinamide *N*-methyltransferase. cDNA cloning, expression, and biochemical characterisation. J. Biol. Chem. 269, 14835–14840.

Allali-Hassani, A., Pan, P.W., Dombrovski, L., Nainanovich, R., Tempel, W., Dong, A., Loppnau, P., Martin, F., Thornton, J., Edwards, A.M., Bochkarev, A., Plotnikov, A.N., Vedadi, M., Arrowsmith, C.H., 2007. Structural and chemical profiling of the human cytosolic sulfotransferases. PLoS Biol. 5, e97.

Alston, T.A., Abeles, R.H., 1988. Substrate specificity of nicotinamide *N*-methyltransferase isolated from porcine liver. Arch. Biochem. Biophys. 260, 601–608.

Banasik, M., Ueda, K., 1999. Dual inhibitory effects of dimethyl sulfoxide on poly(ADP-ribose) synthetase. J. Enzyme Inhib. 14, 239–250.

Banasik, M., Stedeford, T., Strosznajder, R.P., Persad, A.S., Tanaka, S., Ueda, K., 2004. The effects of organic solvents on poly(ADP-ribose) polymerase-1 activity: implications for neurotoxicity. Acta Neurobiol. Exp. 64, 467–473.

Berman, H.M., Burley, S.K., Kleywegt, G.J., Markley, J.L., Nakamura, H., Velankar, S., 2016. The archiving and dissemination of biological structural data. Curr. Opin. Struct. Biol. 40, 17–22.

Bomati, E.K., Noel, J.P., 2005. Structural and kinetic basis for substrate selectivity in Populus tremuloides sinapyl acohol dehydrogenase. Plant Cell 17, 1598–1611.

Bradbury, A.J., Costall, B., Domeney, A.M., Testa, B., Jenner, P.G., Marsden, C.D., Naylor, R.J., 1985. The toxic actions of MPTP and its metabolite MPP++ are not mimicked by analogues of MPTP lacking an *N*-methyl moiety. Neurosci. Lett. 61, 121–126.

Busby, W.F., Ackermann, J.M., Crespi, C.L., 1999. Effect of methanol, ethanol, dimethyl sulfoxide and acetonitrile on *in vitro* activities of cDNA-expressed human cytochromes P-450. Drug Metab. Dispos. 27, 246–249.

Carr, L.A., Basham, J.K., 1991. Effects of tobacco smoke constituents on MPTP-induced toxicity and monoamine oxidase activity in the mouse brain. Life Sci. 48, 1173–1177.

Chauret, N., Gauthier, A., Nicoll-Griffith, D.A., 1998. Effect of common organic solvents on *in vitro* cytochrome P450-mediated metabolic activities in human liver microsomes. Drug Metab. Dispos. 26, 1–4.

Easterbrook, J., Lu, C., Sakai, Y., Li, A.P., 2001. Effects of organic solvents on the activities of cytochrome P450 isoforms, UDP-dependent glucuronyl transferase, and phenol sulphotransferase in human hepatocytes. Drug Metab. Dispos. 29, 141–144.

Emanuelli, M., Santarelli, A., Sartini, D., Ciavarella, D., Rossi, V., Pozzi, V., Rubini, C., Lo Muzio, L., 2010. Nicotinamide *N*-methyltransferase upregulation correlates with tumour cell differentiation in oral squamous cell carcinoma. Histol. Histopathol. 25, 15–20.

Faulds, C.B., Perez-Boada, M., Martinez, A.T., 2011. Influence of organic co-solvents on the activity and substrate specificity of feruloyl esterases. Bioresour. Technol. 102, 4962–4967.

Gearhart, D.A., Collins, M.A., Lee, J.M., Neafsey, E.J., 2000. Increased β-carboline 9*N*-methyltransferase activity in the frontal cortex in Parkinson's disease. Neurobiol. Dis. 7, 201–211.

Godin, C.S., Crooks, P.A., 1989. *N*-Methylation as a toxication route for xenobiotics. II. *In vivo* formation of *N,N'*-dimethyl-4,4'-bipyridyl ion (paraquat) from 4,4'-bipyridyl in the guinea pig. Drug Metab. Dispos. 17, 180–185.

Han, H., Theriault, J.F., Chen, G., Lin, S.X., 2017. Substrate inhibition of 17β-HSD1 in living cells and regulation of 17β-HSD7 by 17β-HSD1 knockdown. J. Steroid

Biochem. Mol. Biol. 172, 36–45.
Hancock, A.A., Bush, E.N., Stanisic, D., Kyncl, J.J., Lin, C.T., 1988. Data normalisation before statistical analysis: keeping the horse before the cart. Trends Pharmacol. Sci. 9, 29–32.
Hong, E., Kim, G.H., 2013. GC-MS analysis of the extracts from Korean cabbage (*Brassica campestris* L. ssp. *pekinensis*) and its seed. Prev. Nutr. Food Sci. 18, 218–221.
Irwin, I., Langston, J.W., DeLanney, L.E., 1987. 4-Phenylpyridine (4PP) and MPTP: the relationship between striatal MPP + + concentrations and neurotoxicity. Life Sci. 40, 731–740.
Johannesson, H., Denisov, V.P., Halle, B., 1997. Dimethyl sulfoxide binding to globular proteins: a nuclear magnetic relaxation dispersion study. Protein Sci. 6, 1756–1763.
Jung, J., Kim, L.J.Y., Wang, X., Wu, Q., Sanvoranart, T., Hubert, C.G., Prager, B.C., Wallace, L.C., Jin, X., Mack, S.C., Rich, J.N., 2017. Nicotinamide metabolism regulates glioblastoma stem cell maintenance. JCI Insight 18, 90019.
Kim, J., Hong, S.J., Lim, E.K., Yu, Y.S., Kim, S.W., Roh, J.H., Do, I.G., Joh, J.W., Kim, D.S., 2009. Expression of nicotinamide *N*-methyltransferase in hepatocellular carcinoma is associated with poor prognosis. J. Exp. Clin. Cancer Res. 28, 20.
Kim, S., Thiessen, P.A., Bolton, E.E., Chen, J., Fu, G., Gindulyte, A., Han, L., He, J., He, S., Shoemaker, B.A., Wang, J., Yu, B., Zhang, J., Bryant, S.H., 2016. PubChem substance and compound databases. Nucleic Acids Res. 44, D1202–D1213.
Kuper, J., Wong, T.S., Roxxatano, D., Wilmanns, M., Schwaneberg, U., 2007. Understanding a mechanism of organic cosolvent inactivation in heme monooxygenase P450 BM-3. J. Am. Chem. Soc. 129, 5786–5787.
Kwak, G.-H., Choi, S.H., Kim, J.-R., Kim, H.-Y., 2009. Inhibition of methionine sulfoxide reduction by dimethylsulphoxide. BMB Rep. 42, 580–585.
Lin, Y., Lu, P., Tang, C., Mei, Q., Sandig, G., Rodrigues, A.D., Rushmore, T.H., Shou, M., 2001. Substrate inhibition kinetics for cytochrome P450-catalyzed reactions. Drug Metab. Dispos. 29, 368–374.
Matsubara, K., Aoyama, K., Suno, M., Awaya, T., 2002. *N*-Methylation underlying Parkinson's disease. Neurotoxicol. Teratol. 24, 593–598.
Meijers, R., Adolph, H.-W., Dauter, Z., Wilson, K.S., Lamzin, V.S., Cederdren-Seppezauer, E.S., 2007. Structual evidence for a ligand coordination switch in liver alcohol dehydrogenase. Biochemistry 46, 5446–5454.
Parsons, R.B., Smith, M.–L., Williams, A.C., Waring, R.H., Ramsden, D.B., 2002. Expression of nicotinamide *N*-methyltransferase (E.C. 2.1.1.1) in the Parkinsonian brain. J. Neuropathol. Exp. Neurol. 61, 111–124.
Parsons, R.B., Smith, S.W., Waring, R.H., Williams, A.C., Ramsden, D.B., 2003. High expression of nicotinamide *N*-methyltransferase in patients with idiopathic Parkinson's disease. Neurosci. Lett. 342, 13–16.
Parsons, R.B., Aravindan, S., Kadampeswaran, A., Evans, E.A., Sandhu, K.K., Levy, E.R., Thomas, M.G., Austen, B.M., Ramsden, D.B., 2011. The expression of nicotinamide *N*-methyltransferase increases ATP synthesis and protects SH-SY5Y neuroblastoma cells against the toxicity of Complex I inhibitors. Biochem. J. 436, 145–155.
Patel, M., Vasaya, M.M., Asker, D., Parsons, R.B., 2013. HPLC-uv method for measuring nicotinamide *N*-methyltransferase activity in biological samples: evidence for substrate inhibition kinetics. J. Chromatogr. B 921–922, 87–95.
Peng, Y., Sartini, D., Pozzi, V., Wilk, D., Emanuelli, M., Yee, V.C., 2011. Structural basis of substrate recognition in human nicotinamide *N*-methyltransferase. Biochemistry 50, 7800–7808.
Perlman, R.L., Wolff, J., 1968. Dimethyl sulfoxide: an inhibitor of liver alcohol dehydrogenase. Science 160, 317–319.
Perry, T.L., Jones, K., Hansen, S., Wall, R.A., 1987. 4-Phenylpyridine and three other analogues of 1-methyl-4-phenyl-1,2,3,6-tetrahydropyridine lack dopaminergic nigrostriatal neurotoxicity in mice and marmosets. Neurosci. Lett. 75, 65–70.
Plummer, J.M., Greenberg, M.J., Lehman, H.K., Watts, J.A., 1983. Competitive inhibition by dimethylsulfoxide of mulluscan and vertebrate acetylcholinesterase. Biochem. Pharmacol. 32, 151–158.
Smith, M.L., Burnett, D., Bennett, P., Waring, R.H., Brown, H.M., Williams, A.C., Ramsden, D.B., 1998. A direct correlation between nicotinamide *N*-methyltransferase activity and protein levels in human liver cytosol. Biochim. Biophys. Acta 1422, 238–244.
Snyder, S.H., D'Amato, R.J., 1985. Predicting Parkinson's disease. Nature 317, 198–199.
Sperber, H., Mathieu, J., Wang, Y., Ferreccio, A., Hesson, J., Xu, Z., Fischer, K.A., Devi, A., Detraux, D., Gu, H., Battle, S.L., Showalter, M., Valensisi, C., Bielas, J.H., Ericson, N.G., Margaretha, L., Robitaille, A.M., Margineantu, D., Fiehn, O., Hockenbery, D., Blau, C.A., Raftery, D., Margolin, A.A., Hawkins, R.D., Moon, R.T., Ware, C.B., Ruohola-Baker, H., 2015. The metabolome regulates the epigenetic landscape during naïve-to-primed human embryonic stem cell transition. Nat. Cell Biol. 17, 1523–1535.
Thomas, A.F., Bassols, F., 1992. Occurrence of pyridines and other bases in orange oil. J. Agric. Food Chem. 40, 2236–2243.
Thomas, M.G., Saldanha, M., Mistry, R.J., Dexter, D.T., Ramsden, D.B., Parsons, R.B., 2013. Nicotinamide *N*-methyltransferase expression in SH-SY5Y neuroblastoma and N27 mesencephalic neurones induces changes in cell morphology *via* ephrin-B2 and Akt signalling. Cell Death Dis. 4, e669.
Thomas, M.G., Marwood, R.M., Parsons, A.E., Parsons, R.B., 2015. The effect of foetal bovine serum supplementation upon the lactate dehydrogenase assay: important considerations for *in vitro* toxicity analysis. Toxicol. In Vitro 30, 300–308.
Thomas, M.G., Sartini, D., Emanuelli, M., van Haren, M.J., Martin, N.I., Mountford, D.M., Barlow, D.J., Klamt, F., Ramsden, D.B., Reza, M., Parsons, R.B., 2016. Nicotinamide *N*-methyltransferase catalyses the *N*-methylation of the endogenous β-carboline norharman: evidence for a novel detoxification pathway. Biochem. J. 473, 3253–3267.
Thomsen, R., Christensen, M.H., 2006. MolDock: a new technique for high-accuracy molecular docking. J. Med. Chem. 49, 3315–3321.
Tracy, T.S., Hummel, M.A., 2004. Modelling kinetic data from *in vitro* drug metabolism enzyme experiments. Drug Metab. Rev. 36, 231–242.
Trevor, A.J., Castagnoli, N., Jr, Caldera, P., Ramsay, R.R., Singer, T.P., 1987. Bioactivation of MPTP: reactive metabolites and possible biochemical sequelae. Life Sci. 40, 713–719.
Tsitsanou, K.E., Oikonomakos, N.G., Zographos, S.E., Skamnaki, V.T., Gregorious, M., Watson, K.A., Johnson, L.N., Fleet, G.W.J., 1999. Effects of commonly used cryoprotectants on glycogen phosphorylase activity and structure. Protein Sci. 8, 741–749.
Tyapochkin, E., Cook, P.F., Chen, G., 2009. para-Nitrophenyl sulfate activation of human sulfotransferase 1A1 is consistent with intercepting the E.PAP complex and reformation of E.PAPS. J. Biol. Chem. 284, 29357–29364.
van Haren, M.J., Torano, J.S., Sartini, D., Emanuelli, M., Parsons, R.B., Martin, N.I., 2016. A rapid and efficient assay for the characterisation of substrates and inhibitors of nicotinamide *N*-methyltransferase. Biochemistry 55, 5307–5315.
Vander Heiden, M.G., Cantley, L.C., Thompson, C.B., 2009. Understanding the Warburg effect: the metabolic requirements of cell proliferation. Science 324, 1029–1033.
Williams, A.C., Ramsden, D.B., 2005. Autotoxicity, methylation and a road to the prevention of Parkinson's disease. J. Clin. Neurosci. 12, 6–11.
Williams, A.C., Hill, L.J., Ramsden, D.B., 2012. Nicotinamide, NAD(P)(H) and methyl group homeostasis evolved and became a determinant of ageing diseases: hypotheses and lessons from Pellagra. Curr. Gerontol. Geriatr. Res. 2012, 302875.
Williams, P.A., Cosme, J., Ward, A., Angove, H.C., Matack Vinkovic, D., Jhoti, H., 2003. Crystal structure of human cytochrome P450 2C9 with bound warfarin. Nature 424, 464–468.
Wu, B., 2011. Substrate inhibition kinetics in drug metabolism reactions. Drug Metab. Rev. 43, 440–456.
Young, J.Y., Westbrook, J.D., Feng, Z., Sala, R., Peisach, E., Oldfield, T.J., Sen, S., Gutmanas, A., Armstrong, D.R., Berrisford, J.M., Chen, L., Chen, M., Di Costanzo, L., Dimitropoulos, D., Gao, G., Ghosh, S., Gore, S., Guranovic, V., Hendrickx, P.M., Hudson, B.P., Igarashi, R., Ikegawa, Y., Kobayashi, N., Lawson, C.L., Liang, Y., Mading, S., Mak, L., Mir, M.S., Mukhopadhyay, A., Patwardhan, A., Persikova, I., Rinaldi, L., Sanz-Garcia, E., Sekharan, M.R., Shao, C., Swaminathan, G.J., Tan, L., Ulrich, E.L., van Ginkel, G., Yamashita, R., Yang, H., Zhuravleva, M.A., Quesada, M., Kleywegt, G.J., Berman, H.M., Markley, J.L., Nakamura, H., Velankar, S., Burley, S.K., 2017. OneDep: unified wwPDB system for deposition, biocuration, and validation of macromolecular structures in the PDB archive. Structure 25, 536–545.
Zheng, X., Boyer, L., Jin, M., Mertens, J., Kim, Y., Ma, L., Ma, L., Hamm, M., Gage, F.H., Hunter, T., 2016. Metabolic reprogramming during neuronal differentiation from aerobic glycolysis to neuronal oxidative phosphorylation. eLife 5, e13374.